12-2014

Multiple osteochondromas in a 16th–19th century individual from Setúbal (Portugal)

Nathalie Antunes-Ferreira

Eugénia Cunha

Carina Marques

Multiple osteochondromas in a 16th–19th century individual from Setúbal (Portugal)

Nathalie Antunes-Ferreira[1], Eugénia Cunha[2], Carina Marques[3]*

[1]Faculdade de Ciências Sociais e Humanas, Universidade Nova de Lisboa, Instituto Superior de Ciências da Saúde Egas Moniz, CIAS– Research Centre for Anthropology and Health and CRIA–Centro em Rede de Investigação em Antropologia, Lisbon, Portugal.

[2]Departamento de Ciências da Vida, Universidade de Coimbra and CENCIFOR–Centro de Ciências Forenses, Coimbra, Portugal.

[3]Departamento de Ciências da Vida, Universidade de Coimbra and CIAS–Research Centre for Anthropology and Health, Coimbra, Portugal.

Abstract An archaeological survey at the church of Nossa Senhora da Anunciada (Setúbal, Portugal) uncovered the remains of 92 individuals. Historical and archaeological data suggest that the inhumations occurred between 1531 and 1839. The present work reports the pathological features of a mature male individual exhibiting multiple osseous bony projections and bone deformity, mainly affecting the metaphyseal and adjacent diaphyseal regions of the long bones. The macroscopic and the radiological analyses of the lesions suggest multiple osteochondromas as the most probable diagnosis. This is the first archaeological case of this disease known on the Portuguese territory and in southern Europe.

Key words: paleopathology, post-medieval, multiple osteochondromas, benign tumor.

Introduction

An archaeologial survey at the church of Nossa Senhora da Anunciada (Setúbal, Portugal) uncovered a burial site occupied between the 16th and 19th centuries. A male skeleton was retrieved, displaying a set of dry bone and radiological features compatible with a diagnosis of multiple osteochondromas (MO). This work reports the first case of MO recovered from a Portuguese archaeological site, contributing to a better portrayal of the chronological and geographic distribution of MO in the past. Moreover, the

importance of the specimen herein described is the extent and number of lesions, which is in some respects analogous to modern clinical cases.

Osteochondroma (OC) is a "cartilage capped bony projection arising on the external surface of bone containing a marrow cavity that is continuous with that of the underlying bone" (Khurana et al., 2002: 234). It results from excessive chondrocyte proliferation and subsequent cartilagineous ossification at the growth plate (near the groove of Ranvier). As such, OCs develop during the first decade of life and cease after skeleton maturation (Porter and Simpson, 1999; Unni, 2001; Bovée, 2008; Ehara and Khurana, 2010; Wuyts et al., 2014). Osteochondromas can be considered as benign cartilaginous tumors, and one of the most common types of benign bone neoplasms (c. 35–45%) (Porter and Simpson, 1999; Fletcher et al., 2002; Khurana et al., 2002; Bovée, 2008; Ehara and Khurana, 2010). Genetic studies (Porter and Simpson, 1999; Ehara and Khurana, 2010) recognized their neoplastic origin, though some authors still consider them as bone dysplasias (Murphey et al., 2000; Unni, 2001; Waldron, 2009). Osteochondromas can be solitary or multiple (c. 15% of patients), with this latter form termed MOs, a hereditary and autosomal dominant disorder associated with mutations on the genes *EXT1* (8q24) and *EXT2* (11p11–p12) (Unni, 2001; Bovée, 2008; Wuyts et al., 2014). Nowadays the global incidence of MO is aproximately 1:50000 to 1:100000, showing a male predominance (Murphey et al., 2000; Unni, 2001; Khurana et al., 2002; Bovée, 2008; Wuyts et al., 2014).

The medical history of MO can be traced back to 1786, when John Hunter performed the first clinical description of this disease (Stieber et al., 2001), though paleopathological research has provided much earlier evidence of this condition, namely through a skeleton from the middle Bronze Age (c. 1700 BC) in ancient Jericho (Lyall and Mann, 1993). Murphy and McKenzie (2010) recently reviewed the paleopathological publications of MO, compiling 16 cases from a wide geographic (Africa, Americas, Asia and Europe) and chronological range (from the middle Bronze Age to the post-medieval period). However, according to this literature review (Murphy and McKenzie, 2010), the skeleton described herein is the first evidence of this disease in southern Europe.

Materials and Methods

Skeleton 37 was recovered without a coffin or other grave goods from a primary burial at the church of Nossa Senhora da Anunciada, Setúbal, Portugal in 2006. The

chronology of the site was established between 1531 and 1839, based on historical and archaeological data. This site was occupied by a population of low socioeconomic status who were predominantly fishermen.

Among the 92 skeletons exhumed, consisting of 11 subadults and 81 adults (26 males, 46 females, and 9 of unknown sex), skeleton 37 was the only one inhumed in ventral decubitus (orientation East–West). This skeleton presented a fairly good degree of completeness, lacking the left fibula, left patella and left foot bones (Figure 1), yet due to the degree of fragmentation the vertebrae and sacrum were not observable. The right foot had 19.2% (n = 5) of the bones present, while this value was 87.0% (n = 47) for the hands. A total of 11 (45.8%) ribs were observable. Overall, the external bone surface was well preserved and observable.

The sex of skeleton 37 was determined from the morphological characteristics of the skull and pelvis (Buikstra and Ubelaker, 1994; Bruzek, 2002; Walker, 2008), indicating a male individual. The age at death assessment suggests that the individual was older than 30 years of age, because of the closure of all epiphysis, including the sternal extremity of the clavicle (Buikstra and Ubelaker, 1994). The analysis of the sternal end of the 4th rib points to an age interval of 28– 52 years (Işcan et al., 1984). The lower limb lesions have the potential to produce gait alterations, precluding the use of the methods for age at death estimation based on the auricular surface and pubic symphysis metamorphosis. The physiological length of the left femur (386 mm) indicates an aproximate stature of 150 cm (Mendonça, 2000).

Paleopathological analysis of the skeleton was performed by macroscopic observation (aided by a magnifying lens) and measurements using a sliding caliper. Digital radiographic analysis (Orthophos XG5 DS/Ceph from Sirona, 62 kV, 8 mA) of the affected bones was performed at the Clínica de Medicina Dentária, Escola Superior de Ciências da Saúde Egas Moniz.

Results

Skeleton 37 exhibited multiple bony projections, characterized by dense and rounded outgrowths on the external bone surface, mainly located on the metaphyseal and adjacent diaphyseal regions of the long bones (Figure 2, Figure 3, Figure 4, Table 1). The key radiological feature is the presence of well-delimited surface lesions, with both the cortex and marrow cavity showing continuity between the outgrowth and the host bone (Figure 5). These features are characteristic and compatible with the ones observed

in OCs (Greenspan and Remagen, 1998; Unni, 2001; Khurana et al., 2002; Ortner, 2003; Richardson, 2005; Bovée, 2008; Waldron, 2009). The radiographic analysis also revealed the typical flattening of the upper portion of the lesion, accompanied by an area of increased density, which is particularly noticeable on the distal right femur (Figure 5). The dry bone observation of this femoral area shows an irregular defect with darker coloration (Figure 3), which could indicate the presence of the cartilage cap *in vivo*, as also noted by Aufderheide and Rodríguez-Martín (1998) in a description of bone OC. There was also an absence of endosteal scalloping (Figure 5).

A total A total of 46 OCs were observed in the skeleton 37 (Table 1). Two types of OCs were identified, i.e. the sessile type (n = 44), which was characterized by a broad base attached to the cortex; and the pedunculated type (n = 1), where a narrow bone forms a pedicle (Greenspan and Remagen, 1998; Murphey et al., 2000; Waldron, 2009; Wuyts et al., 2014). The sole example of pedunculated OC was detected on the right tibia (Figure 4, Table 1).

The upper limbs had a total of seven tenuous to moderate OCs, i.e. 15.2% (7/46) of the total OCs registered, and their distribution was bilateral for the radius (right: n = 2, left: n = 1), unilateral for the ulna (right: n = 1) and unknown for the hands (n = 3) (Table 1). On the upper limb eburnation were observed at the distal articular surfaces of the left radius and right ulna, on the left and right trapezium, the proximal articulation of the first metacarpals and on the distal articular surface of the third metacarpals, suggesting the presence of degenerative joint disease. Although the fragmentation of the bones precluded a metric analysis, there were no apparent length asymmetries.

The lower limbs account for 80.4% (37/46) of OCs and their severity was particularly marked on the bones that make up the knee joints: 26.1% (12/46) and 15.2% (7/46) for the right and left knees, respectively). The femora alone account for 15 OCs (Table 1). Both extremities of the femora were deformed with widening of the metaphyseal region, being more accentuated on the distal extremity (Figure 3).

All of the lesions were expressive in their dimensions. Furthermore, thickening of the left femoral neck with an angle of c. 137° was observed, indicating coxa valga deformity. The fragmentation of the right femur precluded the assessment of length asymmetries. The tibiae were the second anatomical elements with the highest number of OCs (n = 14). The preferential location was the proximal region. The tibial lesions were moderate to expressive in their size (Figure 4, Table 1). There is also evidence of *genu valgum* on the right knee. On the right fibula all of the OCs (n = 5) were located

on the proximal metaphysis (Figure 4, Table 1). On the right foot, the OCs were detected on three proximal phalanges (Table 1). Thus, the OC distribution was bilateral for the femora (right: n = 9, left: n = 6) and tibiae (right: n = 9, left: n = 5), being more expressive on the right side, and undetermined for the fibula (n = 5) and foot (n = 3). Besides the limbs, the third right rib and the right ischium were affected by OC (Table 1).

Discussion and conclusion

The paleopathological diagnosis entails careful analyses of the morphology and pattern of distribution of the lesions, the age and sex of the individual, and the context from which the specimen was retrieved (Ortner, 2003; Marques et al., 2013).

The lesional pattern of skeleton 37 is characterized by bony projections on the external surface of multiple bones. The most remarkable radiological feature of these outgrowths is the continuity between the cortex and cancellous portion of the host bone with the one of the bony projection. This is a typology of lesion considered as pathognomonic (Murphey et al., 2000) or highly suggestive (Greenspan and Remagen, 1998; Unni, 2001; Richardson, 2005; Wuyts et al., 2014) of OC. Nonetheless, other elements support the diagnosis of MO as the most likely etiology. The external morphology of the lesions is compatible with the presentation of OC. Moreover, on the right femur the lesion exhibits an irregular defect of darker coloration, which was noted by other authors (e.g. Aufderheide and Rodríguez-Martín, 1998) as indicative of the presence of a cartilaginous cap in vivo, a distinctive element of OC (Richardson, 2005; Wuyts et al., 2014). The preferential location of the outgrowths on the metaphyseal and adjacent diaphyseal areas of long bones also supports this diagnosis. These lesions develop on the metaphyseal regions during the individual's growth period and can migrate to the diaphysis along the bone growth (Greenspan and Remagen, 1998; Murphey et al., 2000; Ortner, 2003; Richardson, 2005). In our specimen the severity of lesions was predominant on the lower limb, particularly on the knee. According to the clinical literature, the OC most commonly occurs in the distal femur, proximal tibia and proximal fibula, with these areas affected in c. 70–90% of cases (Greenspan and Remagen, 1998; Murphey et al., 2000; Unni, 2001; Ortner, 2003; Richardson, 2005; Waldron, 2009; Clement and Porter, 2014). The cases detected on the paleopathological record suggests that the bones of the knee are most frequently affected (Murphy and McKenzie, 2010), and the pattern tends to be bilateral or symmetrical (Ortner, 2003;

Wuyts et al., 2014), as observed in our case. Most of the OCs observed in the skeleton 37 were of sessile nature, which is compatible with the clinical (Richardson, 2005) and paleopathological data (Murphy and McKenzie, 2010).

Modern clinical studies suggest that the size (1–10 cm) and number of OCs vary significantly (Murphey et al., 2000; Waldron, 2009; Wuyts et al., 2014). We observed a total of 46 OCs, with a maximum size of 23.8 mm × 40.9 mm ×10.9 mm recorded in the distal part of the left femur. The size, location, number of lesions, and their sessile nature can be correlated with the presence of further skeletal alterations (Porter and Simpson, 1999; Murphey et al., 2000; Clement and Porter, 2014), such as bone deformity and hypertrophy, bone curving and length reduction, shortened stature, coxa valga, knee and ankle valgus, thickening and abnormalities of femoral neck, bone synostosis, and other clinical problems (Murphey et al., 2000; Stieber et al., 2001; Unni, 2001; Noonan et al., 2002; Richardson, 2005; Ehara and Khurana, 2010; Wuyts et al., 2014). The deformities shown in skeleton 37 consisted of widening of the extremities of bones, particularly on the femora, coxa valga and genu valgum. Clinical studies refer to a prevalence of up to 25% of coxa valga and genu valgum in patients with MO (Murphey et al., 2000; Clement and Porter, 2014). Murphy and McKenzie (2010) listed 28.6% (n = 2/7) of coxa valga and 44.0% (n = 4/9) of genu valgum in the cases compiled from the paleopathological record. Shortened stature is a feature often mentioned on both clinical and paleopathological reports, which can occur in c. 40% of the individuals (Richardson, 2005; Murphy and McKenzie, 2010; Wuyts et al., 2014). The 150 cm of stature of skeleton 37 is shorter than the mean of the remaining males of the sample, which is 163.8 cm (SD = 6.4 cm, n = 10). It is also shorter than the male means of 164.3 cm (n = 21) obtained by Cardoso and Gomes (2009) from a compilation of Portuguese samples from the post-medieval period (15th–19th centuries AD) and of 163.2 cm (n = 27783) reported by Padez (2003) for the early 20th century in Portugal. The sex and age at death profiles in our case do not seem to diverge from epidemiological data (Greenspan and Remagen, 1998; Murphey et al., 2000; Richardson, 2005; Bovée, 2008; Wuyts et al., 2014). Although the morphological features of skeleton 37 are consistent with a diagnosis of MO, it is important to perform a differential diagnosis by analyzing other conditions that produce multiple bony projections (Unni, 2001; Richardson, 2005). Both periosteal chondromas and multiple enchondromas display bony projections; however, with these conditions there is a discontinuity between the lesion and the medullary cavity of the host bone through the

intervening cortex. Moreover, enchondromas tend to be located centrally in the bone (Greenspan and Remagen, 1998; Murphey et al., 2000; Silve and Jüppner, 2006; Ehara and Khurana, 2010).Therefore, these conditions are less likely the cause of the alterations observed on skeleton 37. The epiphyseal location of the exostoses on the dysplasia epiphysealis hemimelica (Trevor's disease) also leads us to discount this cause (Murphey et al., 2000; Richardson, 2005; Glick et al., 2007). Myositis ossificans is also ruled out because the bone formations arise at the sites of insertion of muscles, tendons and ligaments, due to localized trauma, and are often found separated from the bone or still joined to it in an irregular and distorted shape. Moreover, the radiological examination reveals no continuity between the cortical and trabecular bone and the lesional tissue (Aufderheide and Rodríguez-Martín, 1998; Ortner, 2003; Richardson, 2005; Waldron, 2009).

A final note can be made regarding skeleton 37's ventral deposition, which is atypical when compared with the remaining individuals from this site or with the archetypal Christian burials (Gonçalves and Santos, 2005). The paleopathological record demonstrated the existence of unusual burials associated with diverse skeletal pathologies or deformities (Gonçalves and Santos, 2005; Tsaliki, 2008). Even if we do not have clear evidence that the lesions of skeleton 37 were apparent during the individual's life or that they induced a social stigma, we can hypothesize that the deformity led to the deviant burial, since MO produce osseous deformities (Murphey et al., 2000; Richardson, 2005) that can impact on the physical, social, and psychological well-being of individuals (Goud et al., 2012).

In sum, we propose MO as the diagnosis of the present specimen based on the morphological and radiological analysis. The present case report is very significant because it extends the known geographical distribution of MO to embrace the Portuguese territory and southern European, according to a literature review (Murphy and McKenzie, 2010). Due to the strong genetic and inherited character of MO a better assessment of its populational distribution would contribute to a better understanding of this disease.

Acknowledgments

This work was undertaken as part of the PhD research by N.A.-F., funded by the Fundação para a Ciência e Tecnologia (Grant No. SFRH/BD/70158/2010). We would like to thank Cooperativa Egas Moniz for the radiographic exam at the Medical Dental

Clinic of Escola Superior de Ciências da Saúde Egas Moniz. We would also like to thank Prof. E. Crubézy for his assistance with the diagnosis, Vitor Matos for fruitful comments and review, and Mrs. Maria Stetin for the English editing.

References

Aufderheide A. and Rodríguez-Martín C. (1998) The Cambridge Encyclopaedia of Human Paleopathology. Cambridge University Press, Cambridge.

Bovée J. (2008) Multiple osteochondromas. Orphanet Journal of Rare Diseases, 3: 3.

Bruzek J. (2002) A method for visual determination of sex, using the human hip bone. American Journal of Physical Anthropology, 117: 157–168.

Buikstra J. and Ubelaker D. (1994) Standards for Data Collection from Human Skeletal Remains: Proceedings of a Seminar at the Field Museum of Natural History. Arkansas Archeological Survey Research Series No 44, Fayetteville, AR.

Cardoso H. and Gomes J. (2009) Trends in adult stature of peoples who inhabited the modern Portuguese territory from the Mesolithic to the late 20th century. International Journal of Osteoarchaeology, 19: 711–725.

Clement N. and Porter D. (2014) Can deformity of the knee and longitudinal growth of the leg bone be predicted in patients with hereditary multiple exostoses? A cross-sectional study. The Knee, 21: 299–303.

Ehara S. and Khurana, J. (2010) Systematic approach to tumors and focal lesions of bone. In: Bonakdarpour A., Reinus W. and Khurana J. (eds.), Diagnostic Imaging of Musculoskeletal Diseases. Springer, New York, pp. 241–311.

Fletcher C., Unni K., and Mertens F. (2002) World Health Organization Classification of Tumours. Pathology and Genetics of Tumours of Soft Tissue and Bone. IARC Press, Lyon.

Glick R., Khaldi L., Ptaszynski K., and Steiner G. (2007) Dysplasia epiphysealis hemimelica (Trevor's disease): a rare developmental disorder of bone mimicking osteochondroma of long bones. Human Pathology, 38: 1265–1272.

Gonçalves M. and Santos A. (2005) Novos testemunhos do sistema defensivo islâmico de Silves e os restos osteológicos humanos encontrados junto à muralha de um arrabalde – notícia preliminar. Xelb, 5: 177–200.

Goud A., Lange J., Scholtes V., Bulstra S., and Ham S. (2012) Pain, physical and social functioning, and quality of life in individuals with multiple hereditary exostoses in the Netherlands: a national cohort study. Journal of Bone & Joint Surgery, 94: 1013–1020.

Greenspan A. and Remagen W. (1998) Differential Diagnosis of Tumors and Tumor-like Lesions of Bone and Joints, 1st edn. Lippincott-Raven, Philadelphia, New York.

Işcan M., Loth S., and Wright R. (1984) Age estimation from rib by phase analysis: white males. Journal of Forensic Sciences, 29:1094–1104.

Khurana J., Abdul-Karim F., and Bovée J. (2002) Osteochondroma. In: Fletcher C., Unni K., and Mertens F. (eds.), World Health Organization Classification of Tumours. Pathology and Genetics of Tumours of Soft Tissue and Bone. IARC Press, Lyon, pp. 234–236.

Lyall H. and Mann G. (1993) Diaphyseal aclasis in citizens of ancient Jericho. International Journal of Osteoarchaeology, 3: 233–240.

Marques C., Santos A., and Cunha E. (2013) Better a broader diagnosis than a misdiagnosis: the study of a neoplastic condition in a male individual who died in early 20th century (Coimbra, Portugal). International Journal of Osteoarchaeology, 23: 664–675.

Mendonça, M. (2000) Estimation of height from the length of long bones in a Portuguese adult population. American Journal of Physical Anthropology, 112: 39–48.

Murphey M., Choi J., Kransdorf M., Flemming D., and Gannon F. (2000) Imaging of osteochondroma: variants and complications with radiologic-pathologic correlation. Radiographics, 20: 1407–1434.

Murphy E. and McKenzie C. (2010) Multiple osteochondroma in the archaeological record: a global review. Journal of Archaeological Sciences, 37: 2255–2264.

Noonan K., Levenda A., Snead J., Feinberg J., and Mih A. (2002) Evaluation of the forearm in untreated adult subjects with multiple hereditary osteochondromatosis. Journal of Bone and Joint Surgery, 84: 397–403.

Ortner D. (2003) Identification of Pathological Conditions in Human Skeletal Remains. Academic Press, London.

Padez C. (2003) Secular trend in stature in the Portuguese population (1904–2000). Annals of Human Biology, 30: 262–278.

Porter D. and Simpson A. (1999) The neoplastic pathogenesis of solitary and multiple osteochondromas. Journal of Pathology, 188: 119–125.

Richardson R. (2005) Variants of exostosis of the bone in children. Seminars in Roentgenology, 40: 380–390.

Silve C. and Jüppner H. (2006) Ollier disease. Orphanet Journal of Rare Diseases, 1: 37.

Stieber J., Pierz A., and Dormans J. (2001) Hereditary multiple exostoses: a current understanding of clinical and genetic advances.The University of Pennsylvania Orthopaedic Journal,14: 39–48.

Tsaliki, A. (2008) Unusual burials and necrophobia: an insight into the burial archaeology of fear. In: Murphy E. (ed.), Deviant Burial in the Archaeological Record. Oxbow Books, Oxford, pp. 1–16.

Unni K. (2001) Cartilaginous lesions of bone. Journal of Orthopaedic Science, 6: 457–472.

Waldron T. (2009) Palaeopathology. Cambridge University Press, Cambridge.

Walker P. (2008) Sexing skulls using discriminant function analysis of visually assessed traits. American Journal of Physical Anthropology, 136: 39–50.

Wuyts W., Schmale G., Chansky H., and Raskind W. (2014) Hereditary multiple osteochondromas [Updated 21 November 2013]. In: Pagon R., Adam M., and Bird T. (eds.), GeneReviews™ [Internet]. University of Washington, Seattle, WA, 1993–2014. Available from http://www.ncbi.nlm.nih.gov/books/NBK1235/

Tables

Table 1. Distribution, type and size of the osteochondromas per anatomical area observed on skeleton 37.

Bone	No. OC	Location (no.)	Type	Size (mm)*
Right radius	2	*Proximal (1)*		
		Anterolateral, neck of the radius	Sessile	6.3 × 6.3 × 1.1
		Distal (1)		
		Medial, diaphysis	Sessile	Undetermined
Left radius	1	Distal, medial, diaphysis	Sessile	18.0 × 7.3 × 7.4
Right ulna	1	Distal, posterior, diaphysis	Sessile	7.6 × 4.5 × 1.0
Hand	3	Diaphysis of the 4th right metacarpal, dorsal (1)	Sessile	1.7 × 5.7 × 1.6
		Diaphysis of the proximal phalanx, dorsal (1)	Sessile	2.5 × 2.6 × 0.8
		Diaphysis of the proximal phalanx, dorsal (1)	Sessile	1.1 × 1.5 × 0.5
Right rib (3rd)	1	Shaft, inferior border (1)	Sessile	9.0 × 7.6 × 7.1
Right os coxae	1	Ischium, posterior surface (1)	Sessile	16.5 × 10.9 × 5.5
Right femur	9	*Proximal (4)*		
		Anterolateral, adjacent to the femoral neck	Sessile	— × 15.0 × 11.8
		Posterior, adjacent to the greater trochanter	Sessile	8.5 × 16.9 × 9.1
		Posterior, adjacent to the greater trochanter	Sessile	12.9 × 10.4 × 4.1
		Posterior, adjacent to the lesser trochanter	Sessile	15.9 × 31.2 × 9.1
		Distal (5)		
		Anterolateral, diaphysis	Sessile	2.7 × 10.5 × 0.3
		Anterolateral, metaphysis	Sessile	8.0 × 26.0 × 0.5
		Anteromedial, metaphysis	Sessile	13.3 × 20.8 × 4.0
		Posterior, metaphysis, adjacent to the lateral condyle	Sessile	19.0 × 30.0 × 16.8
		Posterior, metaphysis	Sessile	9.4 × 6.7 × 2.7
Left femur	6	*Proximal (2)*		
		Anterior, femoral neck	Sessile	10.6 × 17.4 × 5.7
		Posterior, adjacent to the lesser trochanter	Sessile	11.3 × 13.3 × 9.9
		Distal (4)		
		Anterior, metaphysis	Sessile	9.5 × 7.7 × 0.3
		Anteromedial, metaphysis	Sessile	3.8 × 5.1 × 1.9
		Posterolateral, adjacent to the lateral condyle	Sessile	23.8 × 40.9 × 10.9
		Posteromedial, adjacent to the medial condyle	Sessile	25.6 × 32.2 × 2.7
Right tibia	9	*Proximal (8)*		
		Anteromedial, metaphysis	Sessile	6.5 × 7.2 × 0.6
		Medial, metaphysis,	Sessile	7.4 × 11.5 × 5.4
		Medial, metaphysis	Sessile	7.9 × 11.7 × 4.2
		Lateral, metaphysis	Sessile	14.1 × 12.1 × 7.3
		Posterolateral, metaphysis	Sessile	12.9 × 15.5 × 9.1
		Posteromedial, metaphysis	Sessile	13.7 × 38.6 × 9.3
		Medial, diaphysis	Sessile	17.2 × 17.1 × 7.2
		Posterior, diaphysis	Pedunculated	23.8 × 29.8 × 9.8
		Distal (1)		
		Lateral, insertion of the tibiofibular ligament	Sessile	9.5 × 27.0 × 6.4
Left tibia	5	*Proximal (3)*		
		Medial, metaphysis	Undetermined	Undetermined
		Medial, metaphysis	Sessile	6.6 × 6.3 × 1.1
		Medial, metaphysis	Sessile	8.8 × 14.9 × 5.9
		Distal (2)		
		Posterior, metaphysis	Sessile	11.2 × 13.7 × 3.0
		Posterior, metaphysis	Sessile	5.9 × 8.5 × 2.6
Right fibula	5	*Proximal (5)*		
		Medial, metaphysis	Sessile	1.3 × 22.5 × 6.4
		Medial, metaphysis	Sessile	5.4 × 7.2 × 3.8
		Anterior, metaphysis	Sessile	19.2 × 17.9 × 5.9
		Posteromedial, metaphysis	Sessile	12.8 × 20.3 × 7.3
		Lateral, metaphysis	Sessile	4.0 × 5.0 × 3.5
Right foot	3	Proximal, proximal phalanx, dorsal (1)	Sessile	9.2 × 1.3 × 2.3
		Distal, proximal phalanx, dorsal (1)	Sessile	2.5 × 2.3 × 1.3
		Diaphysis of proximal phalanx, dorsal (1)	Sessile	4.4 × 3.5 × 2.2
Total	46			

no., number; OC, osteochondromas.
* Dimensions: lateral-medial × proximal-distal × height.

Figures

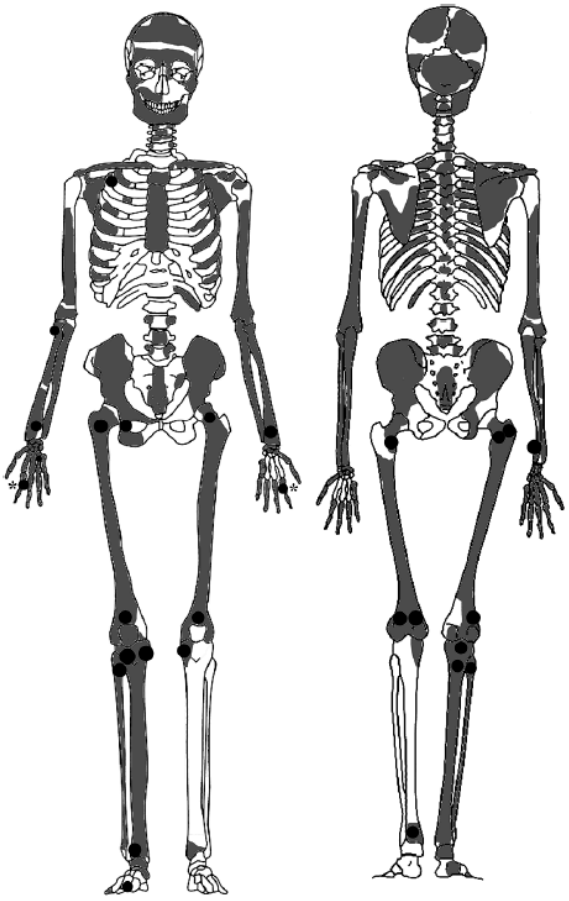

Figure 1. Graphic depiction of the skeleton 37. The grey colour represents the bones present and their completeness. The dark circles indicate the anatomical areas affected by osteochondromas. (*)- Two hand phalanges have osteochondromas, yet their laterality could not be ascertained, thus were here represented on both hands.

Figure 2. Right and left forearm (anterior view), where it can be observed the osteochondromas on both radii (arrows).

Figure 3. Right [(a) anterior and (c) posterior views] and left [(b) anterior and (d) posterior views] femora, exhibiting osteochondromas on multiple locations (arrows). Close up of the affected areas: (e) distal and anterior osteochondromas; (f) proximal and posterior osteochondromas and (g) distal and posterior osteochondromas.

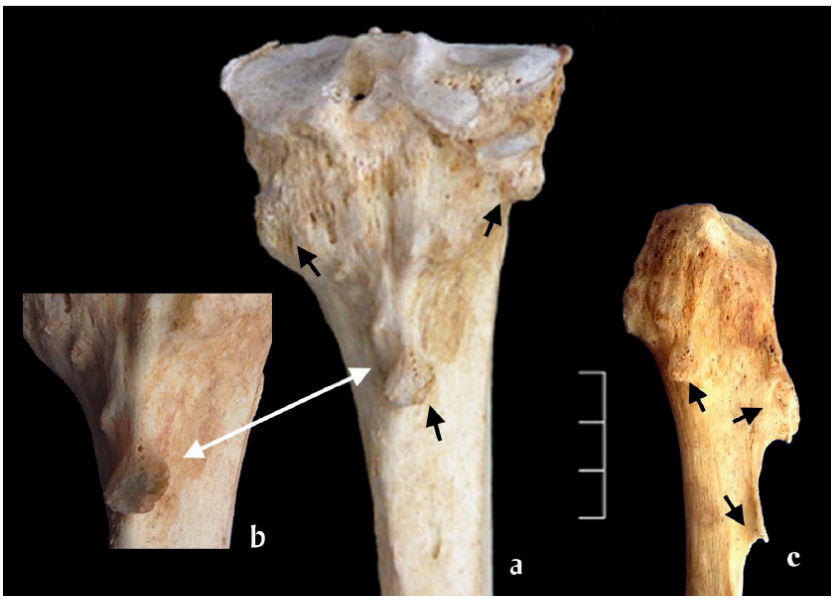

Figure 4. Proximal area of the right tibia [(a)- posterior view] and proximal area of the right fibula [(c)- lateral view] exhibiting osteochondromas (arrows). Close up of pedunculated osteochondroma on the tibia (b).

Figure 5. Radiographic images of the proximal (a) and distal (b) right femur and proximal right tibia (c) (Parameters: 62 Kv, 8 mA).